Johal, N., Arthurs, C., Cuckow, P., Cao, K., Wood, D. N., Ahmed, A., & Fry, C. (2019). Functional, histological and molecular characteristics of human exstrophy detrusor. *Journal of Pediatric Urology*, *15*(2), 154.e1-154.e9. https://doi.org/10.1016/j.jpurol.2018.12.004

Functional, histological and molecular characteristics of human exstrophy detrusor

N Johal[1], C Arthurs[2,4], P Cuckow[1], K Cao[2,4], DN Wood[3], A Ahmed[4], CH Fry[2]

1. Department of Urology, Great Ormond St Hospital for Sick Children, London UK

2. School of Physiology, Pharmacology & Neuroscience, University of Bristol, UK

3. Department of Urology, University College Hospitals, London, UK

4. Centre for Stem Cells and Regenerative Medicine, King's College London, UK

Corresponding author

CH Fry, School of Physiology, Pharmacology & Neuroscience, University Walk, University of Bristol, Bristol BS8 1TD, UK

chris.fry@bristol.ac.uk

Short title: Pathophysiology of human exstrophy detrusor

Extended summary

Introduction. Bladder exstrophy is a congenital anomaly involving fetal exposure and protrusion of the open bladder through an incomplete lower abdominal wall. Techniques to surgically correct exstrophy after birth have greatly improved, but it still presents a major challenge to achieving continence and a good quality of life for patients and their families as the pathophysiology of bladder dysfunction is unknown.

Objectives. A multimodal approach was used to characterise the histological and biomechanical properties of exstrophy detrusor. These were correlated with myocyte responses to agonists and an evaluation of developmental signalling pathways to evaluate the cause of bladder dysfunction in exstrophy.

Study design. Detrusor muscle specimens were obtained during corrective surgery from four exstrophy groups: neonatal (1-3 days, *n*=8), younger children (7months-5 years, *n*=13) and older children (8-14 years, *n*=11) undergoing secondary procedures and cloacal exstrophy (16 days-9 years, *n*=9); control specimens were obtained from children (3 months-9 years, *n*=14) undergoing surgery for other pathologies but with normal bladder function. Five lines of experiments were undertaken: measurement of connective tissue to detrusor muscle ratio, contractile responses to electrical and agonist stimulation; *in vitro* biomechanical stiffness, intracellular Ca^{2+} responses to contractile agonists and immunohistochemistry for proteins (MMP-7, cyclinD1, ß-catenin and *c-myc*) involved in fibrosis generation. Exstrophy data were compared to those from the control group.

Results. Exstrophy tissue demonstrated reduced smooth muscle compared to connective tissue, reduced contractile responses and greater mechanical stiffness. However, intracellular Ca^{2+} responses to agonists were maintained. These changes were greatest in neonatal and cloacal exstrophy samples and least in those from older paediatric bladders. Immunolabelled MMP-7, ß-catenin and *c-myc* were reduced in exstrophy samples.

Discussion. These results highlight the reality that newborns with exstrophy have significantly reduced compliance and bladder underactivity, which may persist or return to normal values with surgery and age. The primary cause of underactivity is increased connective tissue in relation to detrusor muscle, however detrusor myocyte function remains normal. Finally, the increase of smooth muscle content in the paediatric bladder group indicates a remodelling response of the bladder to surgical correction and time. Excess gestational fibrosis is associated with changed expression of key proteins in the *Wnt*-signalling pathway, a potential aetiological factor and therapeutic target.

Conclusion. Results point to connective tissue deposition as the primary pathological process that determines bladder function with normal myocyte function. Future research that reduces connective tissue deposition may lead to improvement in outcomes for these children.

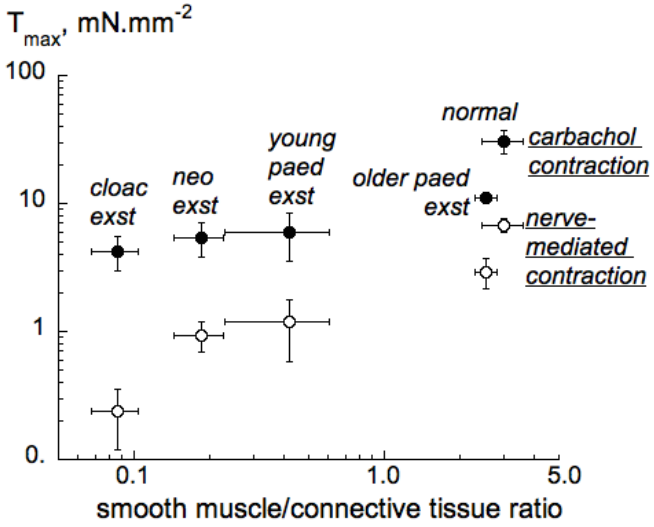

Keywords: human detrusor, exstrophy, contractile function, intracellular [Ca^{2+}], detrusor stiffness

Introduction

Bladder exstrophy is part of the exstrophy-epispadias complex whereby developmental failure of the lower abdominal wall *in utero* leads to a bladder that remains pathologically open and protruding: the prevalence is 3 per 100,000 live births [1]. After neonatal closure, further reconstructive surgery achieves continence, and functional and cosmetically acceptable genitalia. The Kelly procedure [2] is performed at Great Ormond Street Hospital for Children, but in other specialist centres, single and staged-repair techniques are used. Despite successful reconstruction many patients continue with low-capacity bladders with insufficient contractile function [3,4], although a retrospective review of 13 patients following complete primary repair showed good functional recovery [5].

Characteristic of bladder exstrophy [6,7] is increased bladder wall collagen and denervation [8]. Increased collagen results from transformation of several cell types, particularly fibroblasts and epithelia, into myofibroblasts [9]; as well as reduced matrix metalloproteinase (MMP) expression and enhanced expression of tissue inhibitor of metalloproteinases (TIMP) [10]. These processes are controlled by transforming growth factor-β (TGF-β) and augmented by release of *Wnt*-ligand proteins to promote myofibroblast differentiation [11], mediated by transcription factors such as β-catenin, c-*myc* and cyclin-D1. Massive parallel sequencing identified coding changes in 50% of exstrophy patients in 19 different *Wnt* genes [12]. However, functional characterisation to support histological and genetic changes is sparse. In this study, we measured contractile and biomechanical properties of detrusor smooth muscle from human exstrophy bladders and characterised changes to the *Wnt*-signalling pathway to identify potential pathways that may be therapeutic targets to reverse associated fibrosis. We tested the hypothesis that more connective tissue at the expense of smooth muscle in the exstrophy bladder is associated with reduced contractile performance and greater biomechanical stiffness, and if the former was associated with functional denervation and

80 smooth muscle failure. We carried out experiments *in vitro* with isolated detrusor samples to
81 measure: smooth muscle and connective tissue content; active force generation; passive stiffness
82 and intracellular Ca^{2+} responses to contractile agonists. We also performed preliminary
83 observations regarding the molecular basis of increased connective tissue deposition by measuring
84 any changes to the *Wnt*-signalling pathway.

85

Methods

Tissue samples, ethics and preparations. Bladder biopsy samples came from five patient groups. A control group (*n*=14; 10 male (M), 4 female (F); 3 months-9 years) with normal bladder function undergoing open bladder surgery (ureteric reimplantation, urachal cyst excision, localised tumour excision). Four exstrophy groups: i) neonatal exstrophy at time of primary bladder closure (*n*=8; 6M, 2F; age 1-3 days); ii) cloacal exstrophy (*n*=9; 3M, 6F; 16 days-9 years); iii) young children receiving secondary procedures (*n*=13; 8M, 5F; 7months-5 years): a Kelly soft tissue reconstruction (*n*=10), redo bladder neck repair with augmentation (*n*=1), bladder neck closure with augmentation (*n*=1) and bladder and abdominal wall closure for covered variant exstrophy (*n*=1); iv) older children receiving secondary procedures (*n*=11; 8M, 3F; 8-14 years) by Kelly repair (*n*=3), bladder neck repair with augmentation (*n*=6) or bladder neck closure (*n*=2).

All samples were from the lateral wall of the bladder dome, with no evidence of adjacent metaplasia in the one case of tumour excision. After ethical approval, the study was accepted by the R&D department, Great Ormond Street Hospital, London, UK. Parents or guardians were given an information sheet and consent obtained at least 24 hours later. Samples were carried in Ca^{2+}-free solution, within 1-2 hours, to the laboratory for immediate use. Serosa and mucosa were removed by blunt dissection, and detrusor strips (1 mm diam; 4-5 mm length) dissected.

Solutions. Functional experiments (36°C) in Tyrode's solution (mM): NaCl, 118; $NaHCO_3$, 24; KCl, 4.0; $MgCl_2$, 1.0; NaH_2PO_4, 0.4; $CaCl_2$, 1.8; glucose, 6.1; Na pyruvate, 5.0; pH 7.4, 5%CO_2,95% O_2. Ca^{2+}-free solution was (mM): NaCl, 132; KCl, 4.0; NaH_2PO_4, 0.4; glucose, 6.1; Na pyruvate, 5.0; HEPES, 10.0, pH 7.4 with 1M NaOH. High-K Tyrode's contained 80 mM KCl, with no osmolality correction. Drugs were diluted from aqueous stocks. Cell isolation used Ca^{2+}-free solution plus (mg/ml): Worthington Type-II collagenase, 20; hyaluronidase-IS, 0.5; hyaluronidase-III, 0.5; antitrypsin-IIS, 0.9; bovine albumin, 5.0 [13]. All chemicals were from Sigma UK.

110 *Active tension recording.* Muscle strips were tied in a horizontal superfusion trough between an
111 isometric force transducer and a fixed hook. Nerve-mediated contractions were elicited by electrical
112 field stimulation (3-s trains, width 0.1ms, frequency 1-40Hz); abolished by 1μM tetrodotoxin.
113 Contractions generated by direct muscle stimulation were elicited by the muscarinic agonist
114 carbachol (0.1-30μM) or the purinergic agonist α,β–methylene ATP (ABMA, 10 μM). The peak
115 increase from baseline tension was recorded and normalised to cross-section area, *a*.

116 *Biomechanical experiments.* Muscle strips were tied between the force transducer and the central
117 pole of a rotary solenoid. Application of a step voltage to the solenoid rotated it to stretch the
118 muscle by up to 1 mm (20% resting length, *L,* i.e. $\Delta L/L$=0.2) for 50 s before returning to the original
119 length. Stretches were in triplicate at 5-min intervals and average values used. Upon stretch
120 tension, *T*, increased followed by partial relaxation (magnitude T_2, time constant τ), to a new steady-
121 state value, T_1 (figure 3A). The elastic modulus, *E*, was calculated from $E=T_1/(a*\Delta L/L)$; units
122 megapascal, MPa=1N.mm^{-2}). Tension (and hence elastic modulus) immediately after a stretch was
123 greater, the component dissipated by viscoelastic relaxation was calculated by $E_2=T_2/(a*\Delta L/L)$.

124 *Measurement of intracellular Ca^{2+}, $[Ca^{2+}]_i$.* Small (1 mm^3) biopsy pieces were gently triturated for
125 up to 20 min in 1ml of cell isolation solution, gently centrifuged, the supernatant decanted and
126 replaced with Tyrode's solution. The Ca^{2+} fluorochrome Fura-2 (5 μM) was added for 20-30 minutes.
127 Myocytes were identified by a spindle-shaped appearance and samples fixed in 4% formalin solution
128 and labelled for smooth-muscle myosin for confirmation. A drop of cell suspension was placed in a
129 heated (36°C) superfusion chamber and $[Ca^{2+}]_i$ measured by alternate (32 Hz) excitation at 340 and
130 380 nm; fluorescent light was collected between 410 and 510 nm. The magnitude of the
131 fluorescence ratio measured at 340 and 380nm excitation, $R_{340/380}$, was a function of $[Ca^{2+}]_i$. The
132 system was calibrated as described previously [13].

133 *Histology*. Portions of the biopsy were placed in 10 % formaldehyde and stored at 4°C. Samples
134 were dehydrated in alcohol, then xylene and paraffin. Sections (5 µm) on TESPA-coated glass slides
135 were stained with Elastin van Gieson (collagen, red; elastin, black; muscle yellow/orange). The
136 proportion of muscle to connective tissue (collagen and elastin) was measured using colour filters
137 on Image-J. Three separate regions (50x50 µm) per section were measured, distant from mucosa or
138 any obvious areas absent of tissue, and the average recorded.

139 *Multi-channel immunofluorescence labelling and quantitative image intensity analyses.* Antibodies
140 for MMP7 (Abcam), cyclin-D1 (Santa Cruz), ß-catenin and *c-myc* (Novacastra/Leica) were optimised
141 for concentration, pH-dependence and antigen retrieval. A Bond maX™ automated system (Leica
142 BioSystems) was used for labelling [14], the researcher was blind to the antibodies used. Antibodies
143 were incubated simultaneously on each section and labelled with secondary fluorescent antibodies;
144 Cy3 (514/565 nm), Cy5 (633/671 nm), FITC (488/517 nm), Cy3.5 (561/617 nm) respectively, as well
145 as the nuclear counter-stain DAPI (405/429 nm). Each section was imaged with a TCS SP8 confocal
146 system (Leica) at 20x (dry objective) and 40x (1.3 NA, oil objective) with a 6x digital zoom and a *z*-
147 step of 0.17µm. High magnification (x63) images were taken from three, randomly selected, areas
148 of each section and analysed using Huygens professional image deconvolution software (Scientific
149 Volume Imaging, Hilversum, NL) [14] using a macro compiled to measure individual intensities.

150 *Data presentation and analysis.* Data are mean±SEM, *N;n*=number of biopsies;preparations.
151 Immunofluorescence data are medians [25,75% interquartiles] as sets were not normally
152 distributed. Significances between multiple data sets used parametric or non-parametric ANOVA,
153 followed by appropriate *post hoc* tests; the null hypothesis was rejected at *p<0.05, **p<0.01,
154 ***p<0.001. Dose-response or force-frequency curves were fitted to: $T=(T_{max}.x_m)/(x_m+k_m)$; where
155 T_{max} is the maximum response at high stimulation frequency (f) or agonist concentration (S); x is the
156 different values of f or S; k_m is the value of x required to achieve $T_{max}/2$; m is a constant. A Spearman

157 correlation coefficient, *r*, tested associations between two variables, for subsequent estimation of

158 a *p*-value.

159

Results

Histology measurements. Figure 1A shows sample sections of detrusor from control and young paediatric exstrophy patients, the latter shows mucosa on the left edge which was avoided for analysis. The ratio of smooth muscle to connective tissue (SM/CT) was measured for all five groups. In all exstrophy cohorts, except the older paediatric cohort, the SM/CT ratio was significantly lower compared to the normal cohort (Table 1). Moreover, there was a progressive and significant decline of the ratio from the control and older paediatric exstrophy groups, through to younger paediatric exstrophy, neonatal and cloacal exstrophy groups (figure 1B).

Contractile responses to nerve-mediated and agonist-induced activation. The frequency-dependence of nerve-mediated contractions from normal and exstrophy bladders was used to determine: maximum tension at high frequencies, $T_{max,n\text{-}m}$, and $f_{1/2}$, the frequency that generates $T_{max,n\text{-}m}/2$ (figure 2A). $T_{max,\ n\text{-}m}$ was reduced in both paediatric, neonatal and cloacal exstrophy groups compared to control; $f_{1/2}$ values were similar in all groups (Table 1). Atropine-resistance, the percentage residual tension after 1μM atropine, was present in all groups (Table 1, not determined in cloacal exstrophy); percentage values were highly variable, with no significant differences between the cohorts, but in all the data were significantly different from zero.

Dose-response curves to the muscarinic agonist, carbachol showed that the maximum response ($T_{max,carb}$) was lower in all four exstrophy groups. However, carbachol potency was greater in both paediatric and the neonatal exstrophy groups, as seen by larger pEC_{50} values (Table 1), statistical analyses were not performed for agonist data from the cloacal exstrophy group, due to the small sample number. A similar pattern was observed in the magnitude of responses to a single concentration (10 μM) of ABMA. Finally, the ratio of the maximum responses to nerve-mediated stimulation and carbachol ($T_{max,n\text{-}m}/T_{max,carb}$) was calculated: a smaller ratio is interpreted as reduced functional innervation; values were similar in all five groups (Table 1). The relationships between

maximum response to nerve-mediated stimulation (closed circles) or carbachol (open circles) as a function of the SM/CT ratio are shown in figure 2B; contraction magnitude diminished as smooth muscle content decreased.

Passive biomechanical properties. The transient and steady-state passive tensile properties of detrusor muscle strips were measured during a 50s stretch by 20% of the resting length ($\Delta L/L$=0.2). Three variables were measured: steady-state tension (T_1, N.mm^{-2}); magnitude of viscoelastic relaxation (T_2, N.mm^{-2}) and the time constant of viscoelastic relaxation (τ, s; figure 3A, Table 2). Three stretches, five minutes apart, were applied; T_1 and T_2 values were significantly greater during the second and third stretches and similar in value to each other; values of τ were similar for all three stretches. Average values from the second and third stretches for each variable are quoted. Measurements from detrusor samples of control, paediatric exstrophy and neonatal exstrophy bladders were made. Data from the older and young paediatric exstrophy groups were combined due to the relatively small number of biopsy samples tested. No data were available for cloacal exstrophy bladders as the biopsy samples were too small.

The value of elastic modulus, E, a steady-state measure of tissue stiffness, was calculated from T_1 values (see Methods). Values of T_1, for the control, paediatric and neonatal exstrophy groups are shown in figure 3B. Exstrophy data were significantly greater than compared to the normal group. T_2 values were smaller than T_1 in all samples, but a similar trend was measured as for T_1 in the three groups: values of τ were similar in all groups. The relationship between the elastic modulus, E and SM/CT ratio (figure 3C) for these groups shows that stiffness increased as the proportion of connective tissue also increased, note the CT/SM ratio is inverted compared to figure 2B.

Intracellular Ca^{2+} regulation. It is unclear from the contractile data if reduction of contractile function from exstrophy patients was in part due to reduced contractile function of individual

myocytes, as well as reduced smooth muscle content. Altered detrusor function was tested by measuring the change of intracellular calcium ($[Ca^{2+}]_i$), in isolated myocytes from normal and exstrophy bladders in response to contractile agonists. $[Ca^{2+}]_i$ was measured in myocytes from cloacal exstrophy bladders, but the small number of cells precluded statistical comparison, but data are shown for comparison. Data from the two paediatric exstrophy groups have been combined as myocytes were isolated from a total of only seven samples (*n*=3, 4 from young and older paediatric exstrophy groups). The resting $[Ca^{2+}]_i$ was similar in myocytes from the remaining groups (Table 2). The changes of $[Ca^{2+}]_i$, $\Delta[Ca^{2+}]_i$, in response to four contractile interventions were recorded: carbachol for muscarinic receptor activation; ABMA for purinergic receptor activation; 80 mM extracellular KCl to depolarise the cell and activate Ca^{2+} channels; caffeine to release Ca^{2+} from intracellular stores. With cells from control bladder samples the rise of $[Ca^{2+}]_i$, $\Delta[Ca^{2+}]_i$, was not significantly different for all interventions. Moreover, $\Delta[Ca^{2+}]_i$ for each intervention was similar in myocytes from paediatric and neonatal exstrophy bladders (Table 2).

Quantitative image intensity analysis. Multichannel immunofluorescence labelling of a normal and paediatric exstrophy samples (figure 4A, parts a, c), along with higher power regions (parts b, d) presented as deconvoluted images, were used for quantitative analysis. Data from nine normal bladder samples and seven exstrophy (five paediatric and two neonatal exstrophy) are shown (figure 4B). The intensity measurements of the different immunolabels demonstrated a reduction of MMP-7 signal (*p*=0.045), and more significant reductions of β–catenin (*p*=0.0037) and *c*-myc (*p*<0.001) in the exstrophy samples; there was no change to cyclin-D1 labelling.

Discussion

Exstrophy and detrusor function. Reduction of the SM/CT ratio in human exstrophy detrusor correlates with similar previous findings [7,8]. The reduced ratio was greatest in neonates with bladder and cloacal exstrophy, with evidence of recovery in older children of the two paediatric exstrophy groups. Recovery of smooth muscle relates either to the closure procedure and/or ageing itself. As the SM/CT ratio reduced, the greater was reduced contractile function, whether elicited by smooth muscle agonists or electrical stimulation of embedded motor nerves. The ratio of force generated either by nerve-mediated stimulation or carbachol exposure was similar in normal and exstrophy cohorts, suggesting detrusor muscle motor innervation itself was not affected by exstrophy. Moreover, there is no detriment to intracellular signalling pathways that regulate intracellular [Ca^{2+}] between the normal and exstrophy groups, as tested by receptor agonists, cell depolarisation (high-K) or intracellular Ca^{2+} release (caffeine). These data confirm previous observations of exstrophy myocytes responding to carbachol and high-K solutions [15], although the reduced basal [Ca^{2+}] in their exstrophy myocytes was not observed here. Thus, in combination with the histological differences in SM/CT content, replacement of smooth muscle with connective tissue is the most likely reason for reduced active force development. Maintained myocyte function with exstrophy is also indicated by similar motility and proliferation in response to growth factors [16].

Another consequence of the increased connective tissue content in exstrophy bladder samples was greater passive stiffness; the SM/CT ratio showed an inverse relationship to passive stiffness. We did not determine the collagen subtype, which is a major component of connective tissue. However, previous work with adult bladder samples has shown that excessive collagen deposition and poorly compliant bladders is associated with a shift from type-I to type-III collagen [17]. The *in vitro* change to a stiffer, less contractile phenotype is consistent with some clinical studies [18]. Moreover, attempts to improve bladder contractile performance with inotropic agents would be less successful

as residual muscle properties are unaltered. Increased connective tissue, associated with reduced metalloproteinase expression and increased expression of tissue inhibitors of metalloproteinases (TIMP) is associated with adult bladder outlet obstruction [19,20], or even raised intravesicular pressures [21]. This suggests decreased expression of enzymes that degrade collagen may contribute to a similar situation in bladder exstrophy. Treatment of post-radiation fibrotic bladders with relaxin reduced connective tissue deposition and recovered cystometric function [22] and this may offer a similar treatment option with bladder exstrophy.

Pathways influencing connective tissue deposition. The *Wnt* pathway, with intracellular Ca^{2+} and transcription factor co-activators as signal transducers, are key in tissue and organ development [23-25]. In particular, *Wnt*-signalling pathways are important in the terminal differentiation of fibroblasts, smooth muscle cells and epithelial cells to collagen-secreting myofibroblasts. There is little work concerned with human neonatal bladder disorders, but genome expression and genome-wide expression studies have implicated changes to *Wnt* signalling pathways in exstrophy [26,27]. Quantitative image intensity analysis showed reduced labelling for β-catenin and *c*-myc, with reduction of the matrix-metalloproteinase, MMP-7. However, expression of cyclin-D1, another target of β-catenin transcription was not significantly altered in exstrophy samples. Little is known about the particular *Wnt*-proteins that regulate normal human bladder development and generation of fibrosis, but down-regulation of Wnt11 is associated with fibrosis in patients with bladder pain syndrome [28]. Overall, downregulation of a *Wnt*-related pathway in a congenital bladder anomaly is a novel observation [29] and may result in increased differentiation into fibroblasts rather than a smooth muscle lineage. Future work targetting molecular signalling pathways such as *Wnt* and TGF-β, which likely underpin this developmental disease, has the potential to develop prognostic and therapeutic targets.

Limitations. Sample availability was limited by the rarity of these conditions and complexity of surgical procedures and statistical analyses were not always possible, especially with the cloacal exstrophy group. It would have been preferable to perform histological, biomechanical and functional studies on each preparation, but in most cases this was not possible. All samples were given an anonymising study code, but researchers were unblinded for functional experiments, as they also retrieved samples. However, histology and immunohistochemistry experiments were undertaken later with researchers now blinded; the code and diagnosis was revealed only after data collection.

Conclusion

This study highlights the critical importance of raised connective tissue content in bladder exstrophy. Exstrophy management has dramatically improved and surgery now provides continence and urethral voiding for many. However, some still fail to achieve continence and the development of therapies is important. Reduced detrusor contractile function with exstrophy is highly correlated with the SM/CT ratio, alongside normal myocyte function. We suggest a molecular explanation for increased CT in terms of reduced *Wnt*-pathway function.

Funding

This work was supported by a research scholarship to Mr Navroop Johal by the Royal College of Surgeons of England and the Children's Research Fund, Liverpool.

References

[1] Jayachandran D, Bythell M, Platt MW, et al. Register based study of bladder exstrophy-epispadias complex: prevalence, associated anomalies, prenatal diagnosis and survival. J Urol 2011; 186: 2056-2060.

298 [2] Kelly JH. Vesical exstrophy: repair using radical mobilisation of soft tissues. Pediatr Surg Int
299 1995; 10: 298–304
300 [3] Woodhouse CR, Redgrave NG. Late failure of the reconstructed exstrophy bladder. BJU Int
301 1996; 77: 590–592.
302 [4] Cuckow P, Desai D, Ryan K. Physiological reconstruction of the lower urinary tract in bladder
303 exstrophy - 10 years' experience with the Kelly operation. J Urol 2010; 183: e210.
304 [5] Borer JG, Starkosha R, Bauer SB, et al. Combined cystometrography and electromyography of
305 the external urethral sphincter following complete primary repair of bladder exstrophy. J Urol 2014;
306 191: 1547-1552.
307 [6] Lee BR, Perlman EJ, Partin AW, et al. Evaluation of smooth muscle and collagen subtypes in
308 normal newborns and those with bladder exstrophy. J Urol 1996; 156: 2034-2036.
309 [7] Slaughenhoupt BL, Mathews RI, Peppas DS, et al. A large animal model of bladder exstrophy:
310 observations of bladder smooth muscle and collagen content. J Urol 1999; 162: 2119-2122.
311 [8] Mathews R, Wills M, Perlman E, et al. Neural innervation of the newborn exstrophic bladder:
312 an immunohistochemical study. J Urol 1999; 162: 506-508.
313 [9] Kendall RT, Feghali-Bostwick CA. Fibroblasts in fibrosis: novel roles and mediators. Front
314 Pharmacol 2014; 5: 1-13.
315 [10] Yang L, Liu R, Wang X, et al. Imbalance between matrix metalloproteinase-1 (MMP-1) and
316 tissue inhibitor of metalloproteinase-1 (TIMP-1) contributes to bladder compliance changes in
317 rabbits with partial bladder outlet obstruction (PBOO). BJU Int. 2013; 112: E391-397.
318 [11] Xu L, Cui WH, Zhou WC, et al. Activation of Wnt/β-catenin signalling is required for TGF-
319 β/Smad2/3 signalling during myofibroblast proliferation. J Cell Mol Med 2017; 21: 1545-1554.
320 [12] Körberg IB, Hofmeister W, Markljung, E et al. Wnt3 involvement in human bladder exstrophy
321 and cloaca development in zebrafish. Hum Mol Gen 2015; 24: 5069-5078.

322 [13] Sui G, Fry CH, Malone-Lee J, et al. Aberrant Ca^{2+} oscillations in smooth muscle cells from
323 overactive human bladders. Cell Calcium 2009; 45: 456-464.
324 [14] Arya M, Thrasivoulou C, Henrique R, et al. Targets of wnt/ß-catenin transcription in penile
325 carcinoma. PloS one 2015; 10: p.e0124395.
326 [15] Suson KD, Stec AA, Shimosa LA, Gearhart JP. Initial characterization of exstrophy bladder
327 smooth muscle cells in culture. J Urol 2012; 188: 1521-1527.
328 [16] Suson KD, Stec AA, Gearhart JP, Shimosa LA. Transforming growth factor-β1 mediates
329 migration
330 [17] Imamura M, Kanematsu A, Yamamoto S, et al. Basic fibroblast growth factor modulates
331 proliferation and collagen expression in urinary bladder smooth muscle cells. Am J Physiol Renal
332 Physiol 2007; 293: F1007-1017.
333 [18] Puri A, Mishra K, Sikdar S, et al. Vesical preservation in patients with late bladder exstrophy
334 referral: histological insights into functional outcome. J Urol 2014: 192: 1208-1214.
335 [19] Peters CA, Freeman MR, Fernandez CA, et al. Dysregulated proteolytic balance as the basis of
336 excess extracellular matrix in fibrotic disease. Am J Physiol 1997; 272: R1960-1965.
337 [20] Yang L, Liu R, Wang X, et al. Imbalance between matrix metalloproteinase-1 (MMP-1) and
338 tissue inhibitor of metalloproteinase-1 (TIMP-1) contributes to bladder compliance changes in
339 rabbits with partial bladder outlet obstruction (PBOO). BJU Int 2013; 112: e391-397.
340 [21] Backhaus BO, Kaefer M, Haberstroh KM, et al. Alterations in the molecular determinants of
341 bladder compliance at hydrostatic pressures less than 40 cm H_2O. J Urol 2002; 168: 2600-2604.
342 [22] Ikeda Y, Zabbarova IV, Birder LA et al. Relaxin-2 therapy reverses radiation-induced fibrosis
343 and restores bladder function in mice. Neurourol Urodyn 2018 May 28. doi: 10.1002/nau.23721
344 [23] Semenov MV, Habas R, Macdonald BT, et al. SnapShot: noncanonical Wnt signaling pathways.
345 Cell 2007; 131: 1378.e1-1378.e2

346 [24] Sugimura R, Li L. Noncanonical Wnt signaling in vertebrate development, stem cells, and
347 diseases. Birth Defects Res C Embryo Today 2010; 90: 243-256.
348 [25] Thrasivoulou C, Millar M, Ahmed A. Activation of intracellular calcium by multiple Wnt ligands
349 and translocation of ß-catenin into the nucleus: a convergent model of Wnt/Ca^{2+} and Wnt/ß-catenin
350 pathways. J Biol Chem 2013; 288: 35651-35659.
351 [26] Qi L, Chen K, Hur DJ et al. Genome-wide expression profiling of urinary bladder implicates
352 desmosomal and cytoskeletal dysregulation in the bladder exstrophy-epispadias complex. Int J Mol
353 Med; 27: 755-765.
354 [27] Draaken M, Knapp M, Pennimpede T et al. Genome-wide association study and meta-analysis
355 identify ISL1 as genome-wide significant susceptibility gene for bladder exstrophy. Plos Genetics
356 2015; 11(3): e1005024.
357 [28] Choi D, Han JY, Shin JH, et al. Downregulation of WNT11 is associated with bladder tissue
358 fibrosis in patients with interstitial cystitis/bladder pain syndrome without Hunner lesion. Sci Rep
359 2018; 8: 9782.
360 [29] Halt K, Vainio S. Coordination of kidney organogenesis by Wnt signalling. Pediatr Nephrol
361 2014; 29: 737-744.

Figure legends

Figure 1. **Smooth muscle and connective tissue in normal and exstrophy bladders**. A: van Gieson stain of detrusor samples from normal (upper) and paediatric exstrophy (lower) bladders: orange smooth muscle; red connective tissue. B: The smooth muscle:connective tissue (SM/CT) ratio of the detrusor layer from normal, and the four exstrophy cohorts, ***p<0.001

Figure 2. **Active contractile properties of detrusor from normal and exstrophy bladders.** A: Force-frequency curves of nerve-mediated contractions from control and young and old paediatric (paed), neonatal (neo) and cloacal (cloa) exstrophy bladders. Estimation of $T_{max,n\text{-}m}$ and $f_{1/2}$ values are shown for the control bladder curve. B. The association between the SM/CT ratio and either the T_{max} for nerve-mediated contractions ($T_{max,n\text{-}m}$, open circles) or for maximum carbachol contractions ($T_{max,carb}$, closed circles).

Figure 3**.** **Biomechanical characteristics of detrusor from normal and exstrophy bladders.** A: Tracing of isometric force for a stretch of 1 mm for 50 s, resting muscle length 5 mm. B: values of elastic modulus, *E,* for samples from normal, paediatric exstrophy and neonatal exstrophy bladders. ***p<0.001 *vs* normal, ### p<0.001 paediatric *vs* neonatal exstrophy. C: the association between the CT/SM ratio and elastic modulus, *E*, for samples from control, paediatric exstrophy and neonatal exstrophy bladders. Note logarithmic axes in parts B and C.

Figure 4. **Quantitative analysis of *wnt*-related proteins**. A: Representative images (x63) of normal (left) and paediatric exstrophy (right) detrusor. Images a and c: composite overlay of four fluorphores: Cy3 (yellow) for MMP-7; Cy5 (purple) for cyclin-D1; FITC (green) for β-catenin; Cy3.5 (red) for *c-myc*; DAPI nuclear label (blue). Images b,d: higher magnification regions sections to show more clearly individual colour labels B: Quantitative analysis of expression of the four epitopes carried out on grey constructs of images filtered for the four fluorochromes. Median data [25,75% interquartiles], *p<0.05, **p<0.01, ***p<0.001, (N=9;7: control; exstrophy).

386 Figure 1

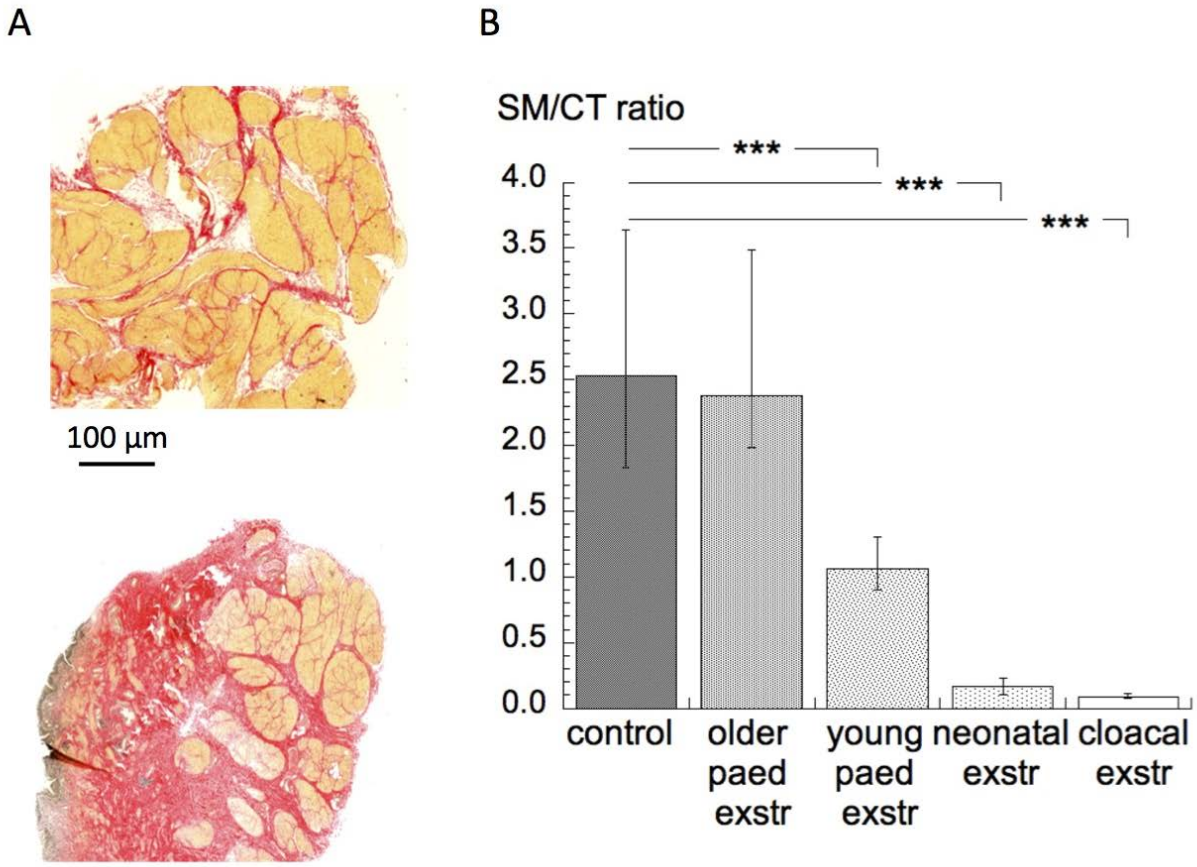

387
388

389 Figure 2

A

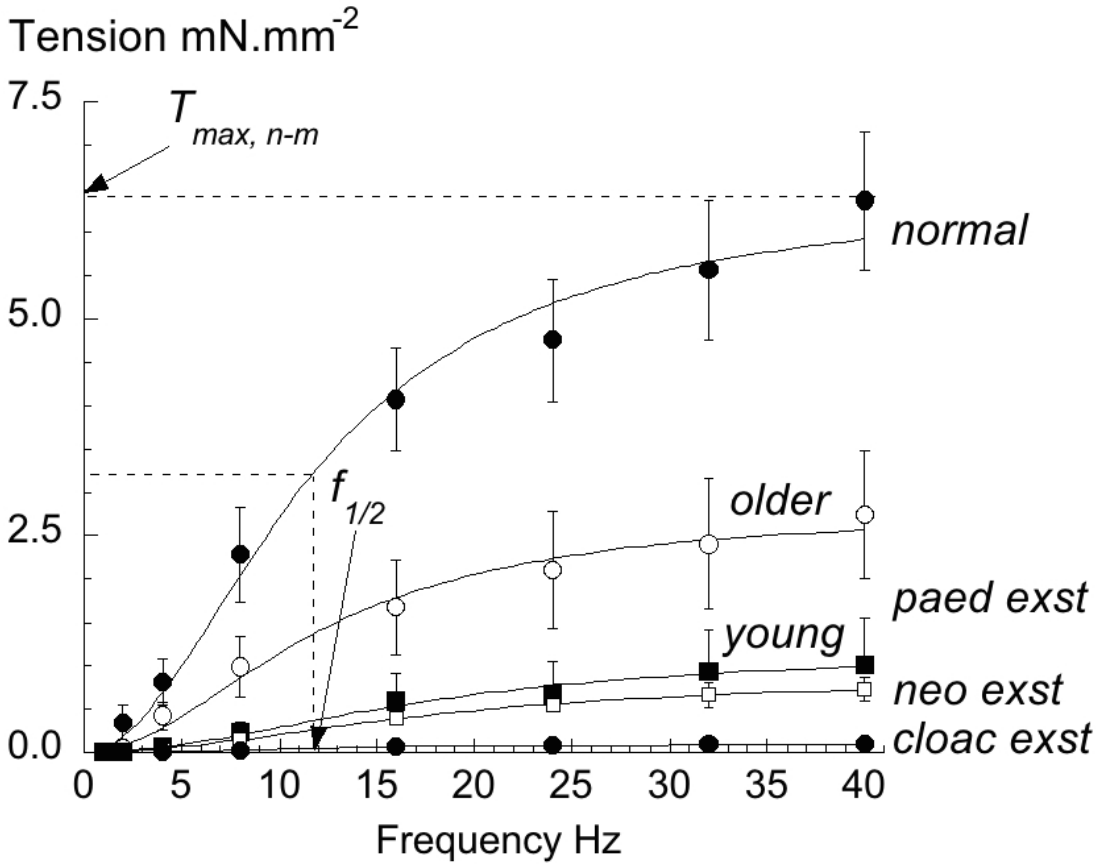
Tension mN.mm-2
7.5
5.0
2.5
0.0
T max, n-m
f 1/2
normal
older
paed exst
young
neo exst
cloac exst
0
5
10
15
20
25
30
35
40
Frequency Hz

B

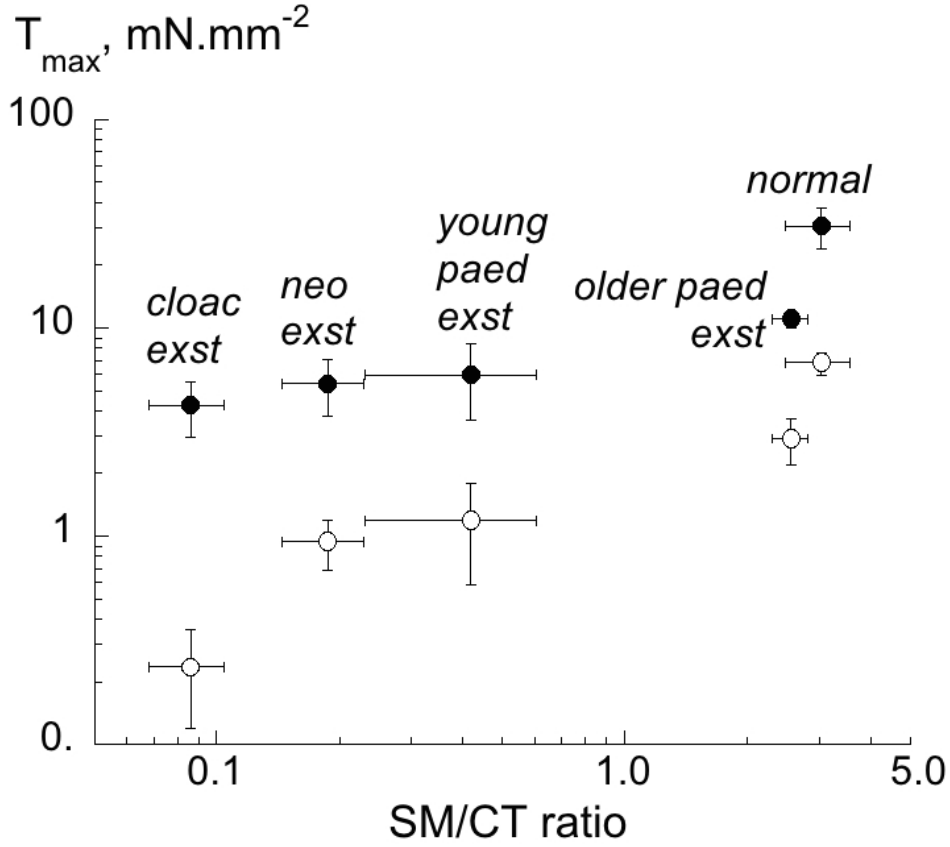
T max, mN.mm-2
100
10
1
0.
cloac exst
neo exst
young paed exst
older paed exst
normal
0.1
1.0
5.0
SM/CT ratio

391 Figure 3

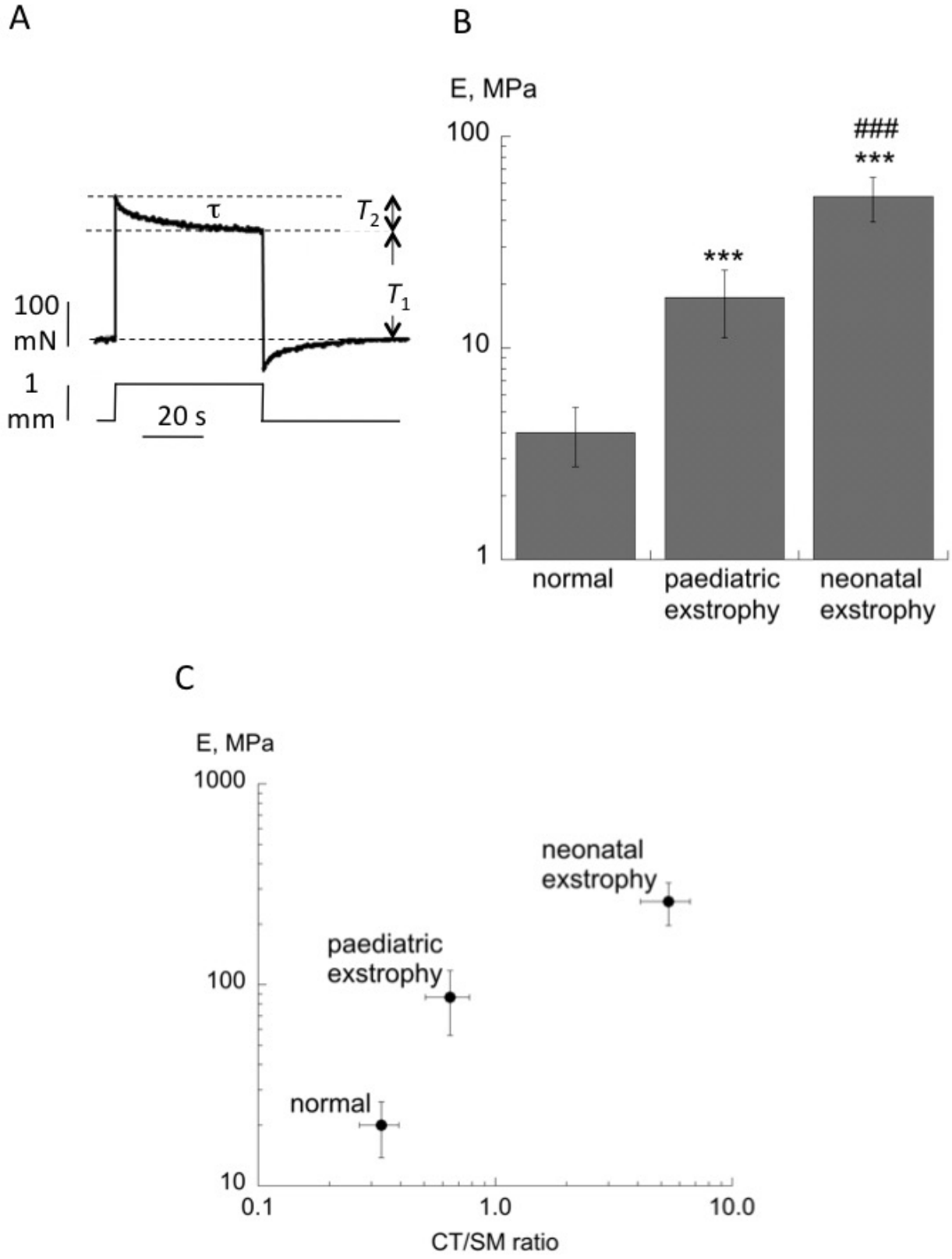

392
393

394 Figure 4

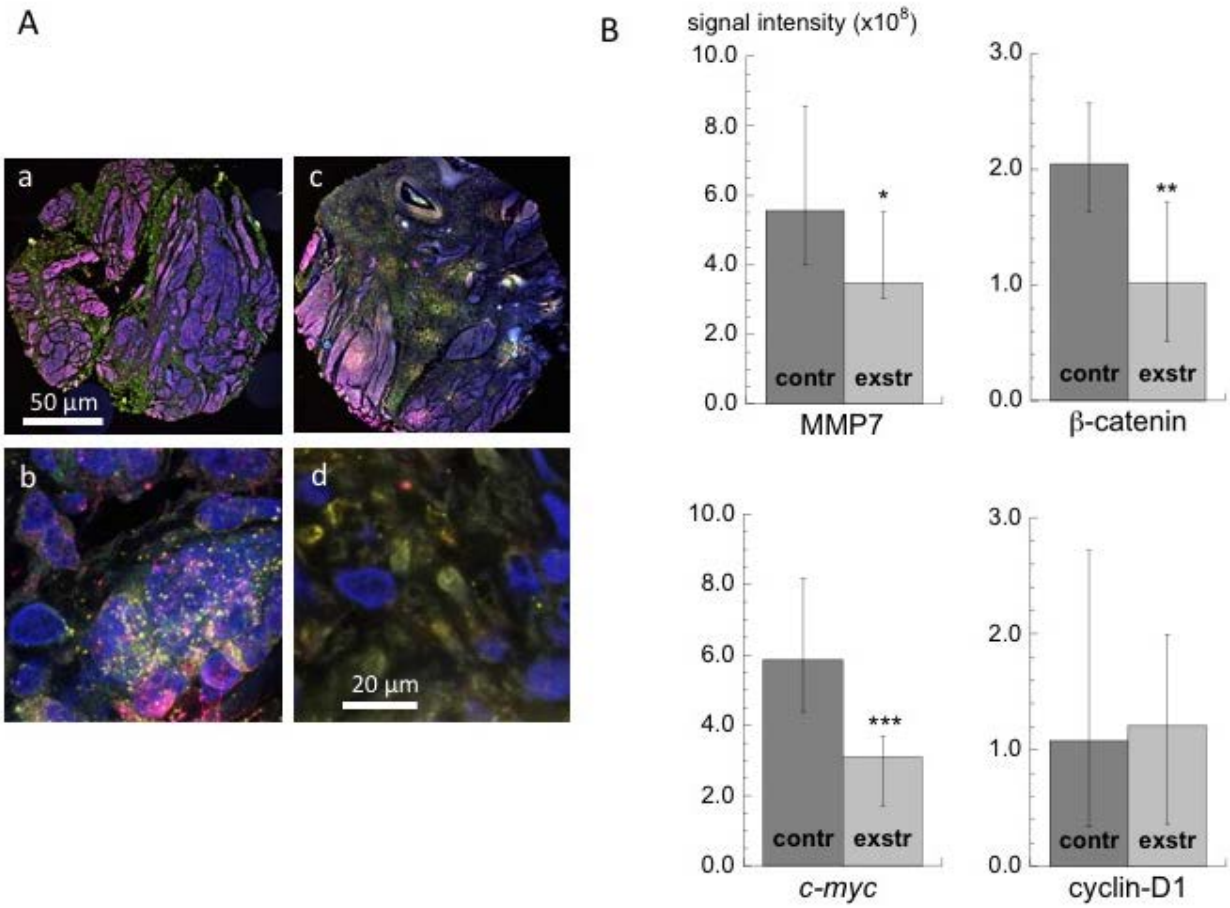

395
396

Table 1. Smooth muscle (SM): connective tissue (CT) ratios and contractile characteristics in detrusor muscle from normal and exstrophy bladders. The paediatric exstrophy data is shown as two sets; from older and younger children (see Methods). Mean data ±SEM (*N* biopsy samples). *p<0.05; **p<0.01; ***p<0.001 *vs* normal.

	Normal	Older Paediatric exstrophy	Young Paediatric exstrophy	Neonatal exstrophy	Cloacal exstrophy
Histology					
SM/CT ratio	3.03±0.56 (11)	2.56±0.26 (6)	0.42±0.19 (10)***	0.19±0.042 (5)***	0.086±0.018 ( )***
Contractile data					
$T_{max,n\text{-}m}$, mN.mm^{-2}	6.80±0.86 (10)	2.93±0.75 (6)*	1.19±0.60 (11)**	0.93±0.25 (5)***	0.24±0.12 (7)***
$f_{1/2}$, Hz	13.2±2.1 (10)	14.2±3.6 (6)	19.4±3.5 (11)	17.2±3.9 (5)	15.6±1.0 (7)
Atropine resist	60.0±28.3 (7)	51.2±14.1 (6)	26.1±8.7 (7)	26.7±17.5 (5)	ND
$T_{max,carb}$ mN.mm^{-2}	30.8±6.68 (10)	11.0±1.01 (6) **	5.98±2.40 (10)***	5.41±1.63 (5)***	4.25, 1.06 (2)
Carb pEC_{50}	5.51±0.04 (10)	6.28±0.12 (6)**	5.99±0.12 (10)**	5.75±0.64 [(5)*	5.67, 5.70 (2)
T_{ABMA}, mN.mm^{-2}	11.2±2.68 (7)	2.02±0.54 (6)***	1.69±0.50 (11)***	0.94±0.22 (5)***	0.05±0.01 (3)
$T_{max,n\text{-}m}/T_{max,carb}$	0.44±0.11 (10)	0.24±0.04 (6)	0.34±0.10 (10)	0.20±0.08 (5)	ND

Table 2. Biomechanics and intracellular [Ca^{2+}] data in detrusor muscle from normal and exstrophy bladders. The paediatric exstrophy data are shown as one data set. Mean data ±SEM (*n* preparations from *N* biopsy samples). *p<0.05. *E*, elastic modulus is used as a measure of detrusor stiffness. E_2 is the viscoelastic component of instantaneous stiffness – see Methods for details.

	Normal	Paediatric exstrophy	Neonatal exstrophy	Cloacal exstrophy
Biomechanics data				
E, MPa (elastic modulus)	20.0±6.20 (9)	86.5±28.1 (6)*	259±61.5 (4)*	
E_2, MPa	6.75±3.60 (9)	20.2±6.60 (6)*	96.0±62.1 (4)*	
τ, seconds	9.6±1.4 (9)	10.8±0.6 (6)	10.4±0.5 (4)	
Intracell [Ca^{2+}] data				
Resting $[Ca^{2+}]_i$, nM	75±16 (9)	111±23 (7)	116±20 (4)	83±9 (3)
$\Delta[Ca^{2+}]_i$ carb, nM	416±100 (9)	432±128 (7)	413±125 (4)	70±12 (3)
$\Delta[Ca^{2+}]_i$ ABMA, nM	361±101 (9)	561±150 (7)	401±65 (4)	118±52 (3)
$\Delta[Ca^{2+}]_i$ KCl, nM	322±94 (9)	419±109 (7)	337±123 (4)	106±37 (3)
$\Delta[Ca^{2+}]_i$ caff, nM	401±120 (4)	469±102 (6)	394±119 (4)	91,171 (2)